



Growth and Characterization of L-Proline Potassium Sulphate (LPPS) - A Semiorganic NLO Crystal

V.Vasantha Kumari^{1*}, P.Selvarajan², R.Thilagavathi¹

¹ Department of Physics, Govindammal Aditanar College for women, Tiruchendur-628215, Tamil Nadu, India.

² Department of Physics, Aditanar College of Arts & Science, Tiruchendur-628216, Tamil Nadu, India.

Abstract: The growth and characterization of semiorganic L-Proline Potassium Sulphate (LPPS) crystal is reported. Single crystals of L-proline potassium sulphate were successfully grown for the first time by solution method with slow evaporation technique at room temperature. Single crystal X-ray diffractometer was utilized to measure the unit cell parameters and to confirm the crystal structure. The planes observed in the powder x-ray diffraction pattern of the grown LPPS crystal have been indexed. The modes of vibration of different molecular groups present in the sample were identified by FTIR spectral analysis and EDAX test was also carried out for confirmation. The optical transmittance window and the lower cut-off wavelength of LPPS have been identified by UV-Vis-NIR studies. Thermal stability of the LPPS was determined by TG/DTA studies. The Vickers microhardness test was also carried out to test the mechanical stability and the hardness parameters were determined. The second harmonic efficiency of the sample was also tested and compared with the standard KDP crystal.

Keywords: Crystal Growth; Single crystal; Characterization; FTIR; TG; microhardness; SHG.

1. Introduction

Nonlinear optics is playing a major role in the emerging photonic and optoelectronic technologies. Extensive studies have been made on the synthesis and crystal growth of new nonlinear optical (NLO) frequency conversion materials because of their potential use in the field of laser technology, optical data storage [1, 2]. Optical nonlinearity of the crystals with O-H bond has been extensively studied [3-5]. In recent years, much attention has been paid to the research of semiorganic crystals. Complexes of amino acids with inorganic salts are promising materials for optical Second Harmonic Generation (SHG) as they tend to exhibit the advantage of the organic amino acids and the inorganic salts [6-9]. Amino acids are interesting materials for NLO applications as they contain donor carboxylic acid (COO⁻) group and the proton acceptor amino (NH₃⁺) group (zwitterions) which create hydrogen bonds in the form of N-H⁺-O-C, which are very strong bonds. Hydrogen bonds have also been used in the possible generation of non-centrosymmetric structures, which is a prerequisite for an effective SHG crystal [10-12]. Proline is an abundant amino acid in collagen and is exceptional among the amino acids because it is the only one in which the amino group is a part of pyrrolidine ring, making it rigid and directional in biological systems [13]. Single crystals of L-proline show no centre of symmetry and their NLO coefficients have been examined by Booma Devi and Dhanasekaran [14]. Some of the L-proline based materials such as prolinium picrate [15], L-proline cadmium chloride monohydrate [16], prolinium tartarate [17], dichlorobis L-proline (zinc II) [18], L-proline lithium chloride monohydrate [19], etc. have been reported. In the present investigation we report the growth of L-proline potassium sulphate and its characterization.

2. Experimental Procedure

2.1 Synthesis and Solubility

The starting material was synthesized by taking L-proline and potassium sulphate in equimolar ratio. The chemical reaction is



The calculated amount of L-proline was first dissolved in deionized water. Potassium sulphate was then added to the solution slowly by stirring for three hours at 50 °C in order to avoid oxidation of the sample. The prepared solution was allowed to dry at room temperature and the salts were obtained by evaporation technique. The synthesized salt of L-proline potassium sulphate (LPPS) thus obtained was subjected to successive re-crystallization to improve the purity. The solubility study was carried out for the re-crystallized LPPS salt in de-ionized water by gravimetric method [20, 21] in the temperature range 30-50 °C. Solubility is defined as the amount of solute in grams present in 100 ml of saturated solution at a particular temperature and it corresponds to saturation between a solid and its solution at given temperature and pressure. A glass beaker with 25 ml of de-ionized water is taken and LPPS salt was added in small amounts at successive stages and stirred continuously. The addition of salt and stirring were continued till a precipitate was formed, which confirmed the supersaturated condition. The 5 ml of the saturated solution was pipetted out and poured into a petridish of known weight. The solvent was completely evaporated by warming the solution at 50 °C. The amount of salt present in 5 ml of the solution is measured by subtracting the empty petridish's weight. From this, the amount of the salt present in 100 ml of the solution was found out. In the same manner, the amount of salt dissolved in 100 ml at 35, 40, 45 and 50 °C was determined. The solubility curve of LPPS salt is presented in Fig. 1. From the graph, it is observed that the solubility of LPPS in water increases with increase in temperature and the sample has positive temperature coefficient of solubility. The positive slope of the solubility curve enables growth of LPPS crystal by slow evaporation method at room temperature.

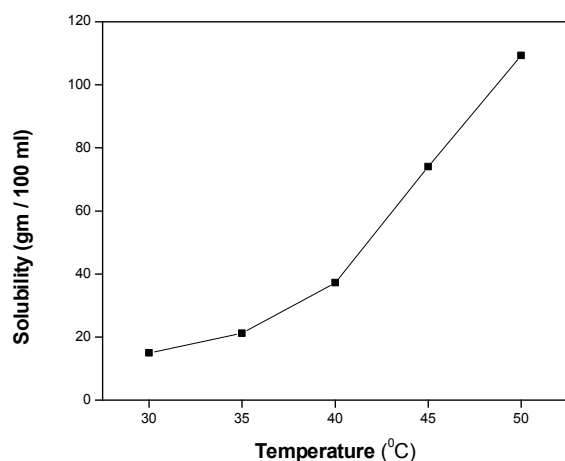


Fig. 1 Solubility curve of LPPS

2.2 Crystal growth

Saturated solution of LPPS was prepared by dissolving the re-crystallized LPPS salt in de-ionized water by continuous stirring of the solution using a magnetic stirrer at room temperature (30°C) in accordance with the solubility data. The saturated solution was filtered with 4 micro Whatmann filter paper and transferred in a beaker. The solution was optimally closed using a perforated sheet and kept in a dust free atmosphere for slow evaporation. Transparent colorless crystals were obtained in a period of 40 days. The photograph of the as grown LPPS crystal is shown in Fig. 2 and the grown crystals are found to be stable, transparent and colorless with well defined crystal faces and edges.

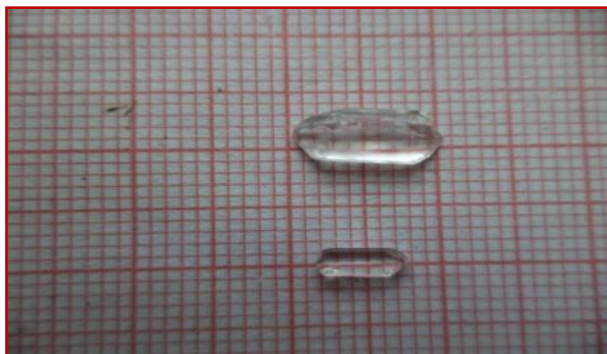


Fig. 2 Photograph of LPPS crystal

2.3 Characterizations

The grown crystals were subjected to single-crystal X-ray diffraction using ENRAF NONIUS CAD-4 Diffractometer, with MoK α radiation ($\lambda=0.71073 \text{ \AA}$). To identify the reflection planes, powder X-ray diffraction pattern of the powdered sample was obtained using a powder X-ray diffractometer (PANalytical Model, Nickel filtered Cu K α radiations with $\lambda=1.54056 \text{ \AA}$ at 35 kV, 10 mA). The sample was scanned over the required range for 2θ values ($10-70^\circ$). The crystalline phase of the sample was identified from the crystallographic parameters such as 2θ , relative intensity and hkl values. The FTIR spectra of LPPS were recorded in KBr phase in the frequency region of $400-4000 \text{ cm}^{-1}$ using a SHIMADZU spectrometer. The transmission spectra was recorded using a Varian Carry 5000 spectrophotometer in the range of $200-2500 \text{ cm}^{-1}$ covering the near ultraviolet, visible and NIR regions. The nonlinear optical conversion efficiencies were tested using a modified setup of Kurtz and Perry. A Q-switched Nd: YAG laser beam of wavelength 1064 nm was used with an input power of 0.68 J. The EDAX spectrum was taken using Jeol 6390LV model scanning electron microscope. The microhardness of the grown crystals was measured using a Leitz Weitzler microhardness tester with a diamond indenter. The well-polished crystal was mounted on the platform of the microhardness tester and loads of different magnitudes (25, 50, 100 g) were applied over a fixed interval of time. The thermogravimetric (TG) analysis of the sample is tested using TGA Q500 V20.10 Build 36 thermal analyser.

3. Results and discussion

3.1 X-ray diffraction analysis

Single crystal X-ray diffraction study was carried out on the as-grown LPPS crystal. The obtained crystallographic data reveals that LPPS crystallizes in orthorhombic structure. The number of molecules per unit cell is 4 and the volume of the unit cell is $430.2(4) \text{ \AA}^3$. The space group of LPPS is found to be $P2_12_12_1$. Since the space group $P2_12_12_1$ is recognized as non-centrosymmetric, there is possibility for second harmonic generation. The crystallographic data of the grown crystal is presented in Table 1.

Table 1 Crystallographic data of LPPS crystal

Parameters	Values
Identification code	LPPS (L-Proline Potassium Sulphate)
Chemical formula	$(C_5H_9NO_2) K_2SO_4$
Molecular weight	289.4 g/mol
Crystal color	Colorless, transparent
Symmetry	Orthorhombic
Space group	$P2_12_12_1$
a	$5.751(4) \text{ \AA}$
b	$7.448(3) \text{ \AA}$
c	$10.042(5) \text{ \AA}$
α	90°
β	90°
γ	90°

Volume	430.2(4) Å ³
Diffractometer	ENRAF NONIUS CAD-4
Radiation wavelength	K _α , 1.54056 Å
Refinement method	Full matrix least square method

The grown LPPS crystal was crushed to a uniform fine powder and subjected to powder X-ray diffraction to identify the reflection planes and hence the crystal parameters. The powder X-ray diffraction pattern of LPPS crystal is shown in Fig. 3. All the reflections of powder XRD pattern were indexed using the INDEXING software package following the procedure of Lipson and Steeple [22]. The obtained h k l values, 2-theta and d-spacing are presented in Table 2. The lattice parameters from powder XRD data were found using UNITCELL software package and the obtained values are found to be a = 5.758 Å, b = 7.4538 Å, c = 10.051 Å. The obtained lattice parameters are in agreement with the single crystal XRD values.

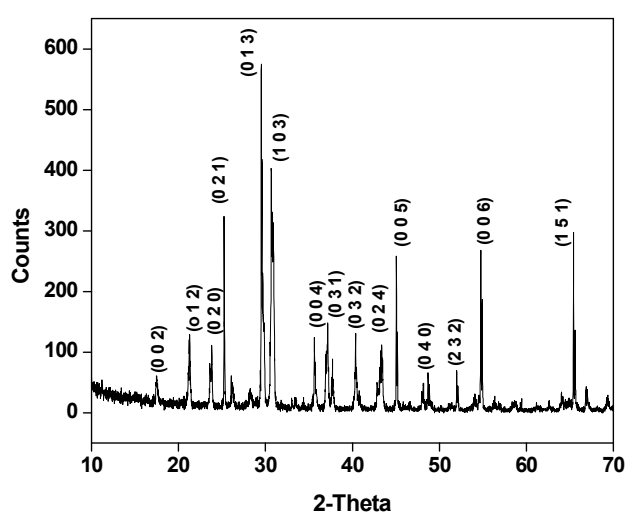


Fig. 3 Powder X-ray diffraction pattern of LPPS

Table 2 Crystallographic parameters of LPPS

Peak No.	2θ	θ (degree)	d (Å)	h k l	Relative intensity (%)
1.	17.650	8.825	5.021	0 0 2	8
2.	21.325	10.662	4.163	0 1 2	21.6
3.	23.875	11.937	3.724	0 2 0	18.4
4.	25.490	12.745	3.492	0 2 1	56
5.	29.227	14.613	3.053	0 1 3	100
6.	30.884	15.442	2.893	1 0 3	69.6
7.	35.737	17.868	2.510	0 0 4	21.6
8.	37.279	18.639	2.410	0 3 1	24.8
9.	40.501	20.250	2.225	0 3 2	22.4
10.	43.436	21.718	2.082	0 2 4	19.2
11.	45.106	22.553	2.008	0 0 5	46.4
12.	48.874	24.437	1.862	0 4 0	10.4
13.	51.912	25.956	1.760	2 3 2	12
14.	54.806	27.403	1.674	0 0 6	48.33
15.	65.321	32.660	1.427	1 5 1	51.2

3.2 FTIR spectral analysis

Fourier Transform Infrared (FTIR) spectrum of the grown LPPS crystal is displayed in Fig. 4. The asymmetric stretching of N-H gives rise to the absorption band at 3448.22 cm^{-1} . The peak observed at 3347.23 cm^{-1} is due to the O-H stretching vibration of LPPS. N-H stretching and out of plane deformation occur at 3177.03 cm^{-1} and 773.75 cm^{-1} . The absorption peaks at 2957.75 cm^{-1} and 1329.57 cm^{-1} corresponds to the stretching and wagging vibrations of CH_2 groups present in the compound. C-N stretching and C-H out of plane deformation occur at 1039.73 cm^{-1} and 950.40 cm^{-1} . The sharp absorption observed at 1650.44 cm^{-1} is due to the NH_2 asymmetric stretching vibration. Stretching and rocking vibrations of COO^- occur at 1410 cm^{-1} and 516.85 cm^{-1} . The peaks at 1361.89 cm^{-1} and 871.89 cm^{-1} are due to the C-C stretching and C-C-N asymmetric vibration of LPPS. The presence of sulphate group present in the sample is confirmed by the presence of SO_4 stretching vibration at 615.24 cm^{-1} . The absence of strong IR band at 1700 cm^{-1} indicates the existence of COO^- in zwitterionic form [19]. The assignments for the characteristic frequencies are given in accordance with the data reported in the literature [20, 23-26] and the complete FTIR spectral data for LPPS crystal are provided in the Table 3.

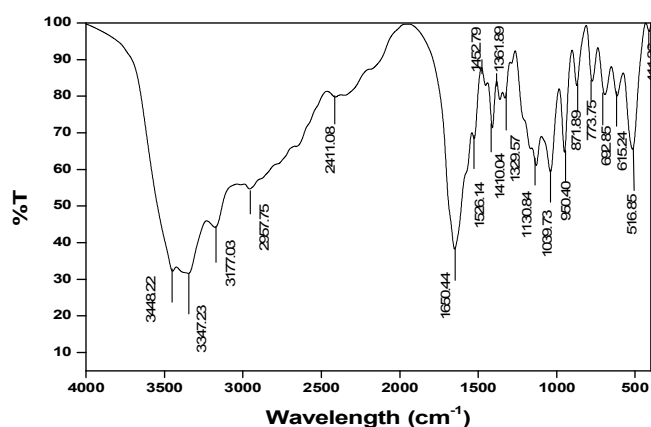


Fig. 4 FTIR spectrum of LPPS crystal

Table 3 FTIR spectral assignments of LPPS

Wave number (cm^{-1})	Assignments
3448.22	N-H asymmetric stretching
3347.23	O-H stretching
3177.03	N-H stretching secondary
2957.75	CH_2 stretching
1650.44	NH_2^+ asymmetric stretching
1410.04	COO^- stretching
1361.89	C-C stretching
1329.57	CH_2 wagging
1039.73	C-N stretching
950.40	C-H out of plane deformation
871.89	C-C-N symmetric stretching
773.75	N-H out of plane bending
615.24	SO_4 stretching
516.85	COO^- rocking

3.3 EDAX analysis

Energy Dispersive X-ray spectroscopy (EDAX) is an analytical technique used for the elemental analysis of the sample. The EDAX analysis of the grown LPPS crystals was carried out and the spectrum is shown in Fig. 5. The peaks in the spectrum confirm the presence of elements C, O, K and S in the sample.

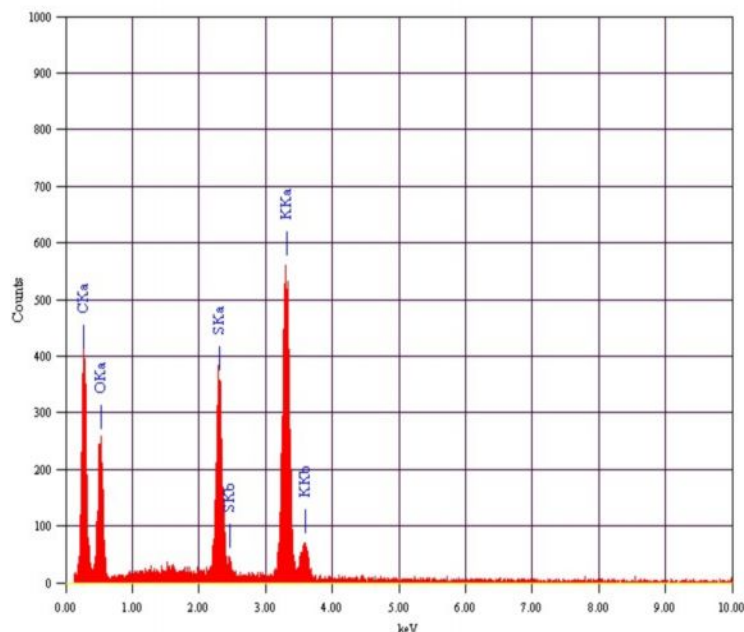


Fig. 5 EDAX spectrum of LPPS

3.4 Thermal analysis

Thermal analysis was carried out for the sample by heating it at a rate of 10 K min^{-1} in inert nitrogen atmosphere. The initial mass of the sample is 6.0 g. It is observed that there is no change in mass up to 360°C and the crystal is found to be stable. The first weight loss occurs at 360°C . The decrease in mass may be due to the thermal decomposition of the elements present in the sample. Minor weight losses occur at 420°C and 450°C . The mass changes in the TG curve are confirmed by DTG peaks shown in Fig. 6. Almost 98% of the sample remains stable up to 800°C . This shows that the grown crystal is thermally stable and makes it suitable for possible applications in lasers where the crystal is required to withstand high temperatures.

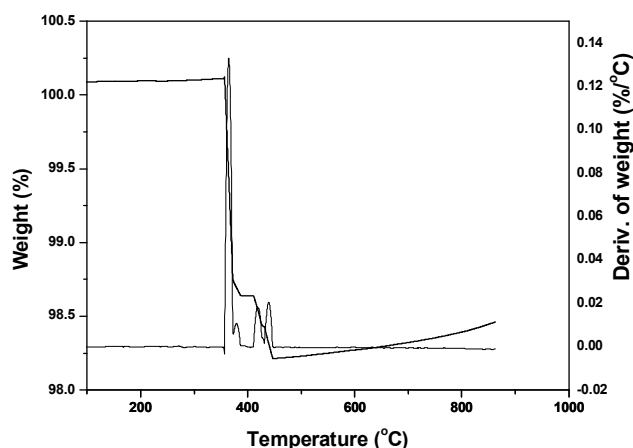


Fig. 6 TG spectrum of LPPS

3.5 Optical transmittance of LPPS

The optical transmittance spectrum of LPPS is shown in Fig. 7. Optically transparent single crystal of thickness about 2 mm was used for this study. There is no appreciable absorption of light in the entire visible range as in the case of all amino acids. This shows the absence of any overtones and absorbance due to electronic transitions above 500 nm. The sharp wavelength cutoff at 256 nm corresponds to the fundamental

absorption in the UV region. Transparent nature in the visible region is an important property for any NLO material from device point of view. The transmittance in the visible region is approximately 84%. Absorption in the near ultraviolet region arises from in connection with the theory of electronic structure, which predicts that the band structure is mostly affected near the band extreme. The absence of absorption in the region between 256 and 1100 nm shows that these crystals are useful for the SHG generation.

Optical absorption coefficient (α) was calculated using the following relation

$$\alpha = \frac{1}{t} \log\left(\frac{1}{T}\right) \quad \text{----- (2)}$$

where T is the transmittance and t the thickness of the crystal. As an indirect band gap material, the crystal under study has an absorption coefficient (α) obeying the following relation for high photon energies ($h\nu$)

$$(\alpha h\nu)^2 = A (h\nu - E_g) \quad \text{----- (3)}$$

where E_g is optical band gap of the crystal and A is a constant. A plot of variation of $(\alpha h\nu)^2$ versus $h\nu$ is shown in Fig. 8. The value of band gap energy was estimated by extrapolating the linear portion to zero absorption. The band gap energy is thus calculated as about 4.7 eV for the LPPS crystal. As a consequence of wide band gap, the grown crystal has a large transmittance in the visible region.

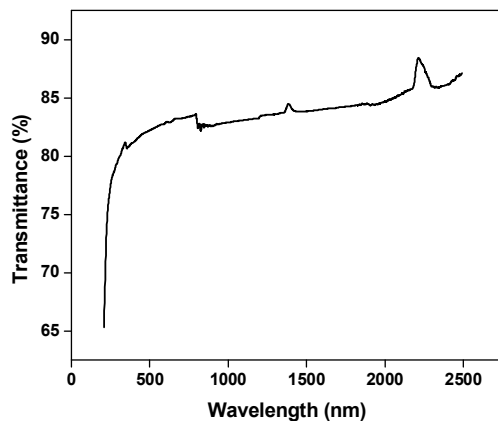


Fig. 7 Optical transmittance of LPPS

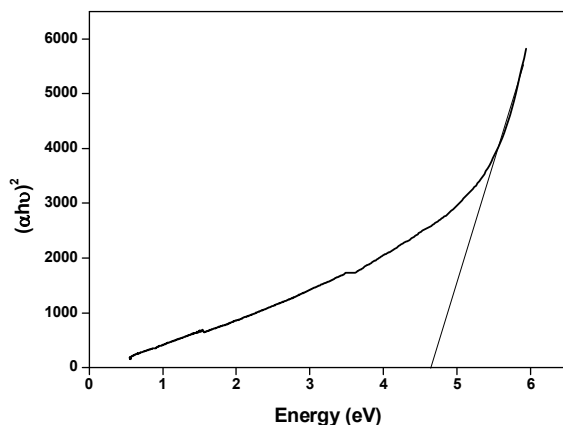


Fig. 8 Plot of $(\alpha h\nu)^2$ versus $h\nu$

The optical properties of the crystals are governed by the interaction between the crystal and the electric and magnetic fields of the electromagnetic wave. Extinction coefficient is the fraction of light lost due to scattering and absorption per unit distance in a participating medium. In electromagnetic terms, the extinction coefficient can be explained as the decay or damping of the amplitude of the incident electric and magnetic fields. The extinction coefficient (K) can be obtained from the relation [18]

$$K = \frac{\lambda\alpha}{4\pi} \quad \text{-----} \quad (4)$$

From the graph (Fig.9) it is clear that the extinction coefficient K varies with wavelength and hence depends on photon energy. Hence by tailoring the photon energy one can achieve the desired material for device fabrication [28].

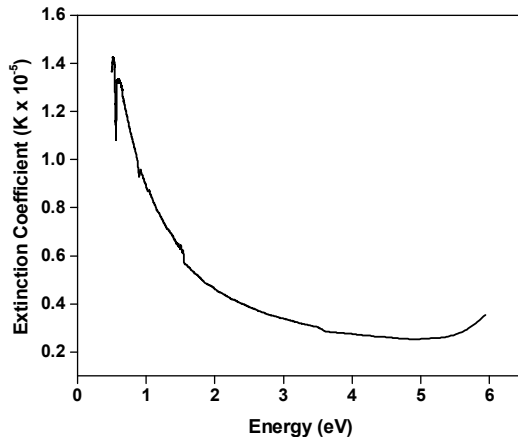


Fig. 9 Plot of Extinction Coefficient versus Energy

3.8 SHG measurement

Second harmonic generation (SHG) test is important to check whether a sample is NLO active or not and it was carried out by powder Kurtz and Perry technique [16]. The crystal was ground into a homogenous powder and densely packed between two transparent glass slides. A Q-switched Nd: YAG laser beam of wavelength 1064 nm (pulse width 6 ns) was allowed to strike the sample cell normally. With this source radiation, the generation of second harmonics was confirmed by the emission of green light from the sample. Second harmonic output of 5.9 mJ was obtained for an input energy of 0.68 J. A sample of powdered potassium dihydrogen phosphate (KDP) was used as the reference material in the SHG measurement and the output was found to be 8.8 mJ. The SHG efficiency for LPPS crystal is found to be 0.67 times that of KDP sample.

3.9 Microhardness analysis

Hardness is one of the important mechanical properties of solid material and microhardness test is one of the best methods to understand the mechanical properties of materials. Transparent crystals free from cracks were selected for microhardness measurements. Before indentation the crystals were carefully lapped and washed to avoid surface effects. The crystal was then subjected to Vicker's microhardness test. The Vicker's microhardness test revealed that the hardness number of LPPS is 86.85 kg/mm² and above which cracks develop on the smooth surface of the crystal due to the release of internal stress generated locally by indentation. The hardness of the crystal indicates that it can be used in device fabrication. The Vicker's hardness number H_v indicates that it can be used in device fabrication. The Vicker's hardness number H_v is calculated using the relation

$$H_v = 1.8544 \frac{P}{d^2} \text{ (kg/mm}^2\text{)} \quad \text{-----} \quad (5)$$

where d is the diagonal length of the indentation and P is the applied load in gram. The variation of H_v for various loads is shown in Fig. 10.

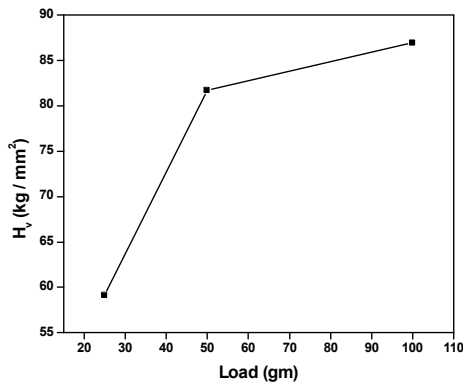


Fig. 10 Plot of load versus H_v

According to normal indentation size effect (ISE), microhardness of crystals decreases with increasing load and in reverse indentation size effect (RISE), the hardness value increases with increasing load. In LPPS, H_v increases with increase in load up to 100 gm, hence exhibiting reverse ISE effect. The traditional Meyer’s law, which gives the relationship between load P and size d, is

$$p = k_1 d^n \tag{6}$$

Where the exponent n in the Meyer’s number and A is a constant. For normal ISE behavior the exponent $n < 2$. When $n > 2$, there is reverse ISE behaviour and when $n = 2$, the hardness is independent of applied load. According to Onitch and Hannemann, [28 - 30], if the value of n is between 1 and 1.6, the material is hard and if it is greater than 1.6 the material is soft. Fig. 11 shows the plot of log P versus log d. The straight line in the graph shows its agreement with Meyer’s law. From the plot, the value of n is found to be 2.85. Hence LPPS belongs to soft material category.

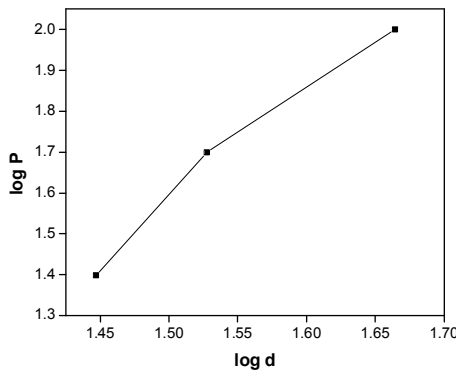


Fig.11 Plot of log P versus log d

According to Meyer’s law,

$$p = k_1 d^n \tag{7}$$

where k_1 is the standard hardness found out from P versus d^n graph (Fig. 12). It is known that the material takes some time to revert to elastic mode after the applied load is removed. So a correction x is applied to the observed d value. Meyer’s law may be modified as

$$p = k_2 (d + x)^2 \tag{8}$$

Simplifying equations (7) and (8), we get

$$d^{n/2} = \left(\frac{k_2}{k_1}\right)^{1/2} d + \left(\frac{k_2}{k_1}\right)^{1/2} x \tag{9}$$

The slope of $d^{n/2}$ versus d (Fig. 13) yields $(k_2/k_1)^{1/2}$ and the intercept is a measure of x .

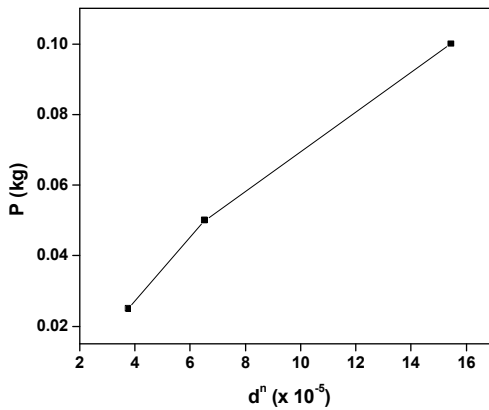


Fig. 12 Plot of P versus d

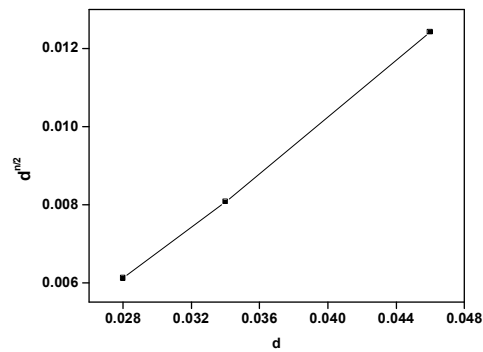


Fig. 13 Plot of $d^{n/2}$ versus d

From the hardness value, the yield strength (σ_v) which is the stress that the material can withstand without permanent deformation can be calculated using the relation [31, 32]

$$\sigma_v = \frac{H_v}{2.9} \left((1 - (n - 2)) \left(\frac{12.5(n-2)}{1-(n-2)} \right)^{n-2} \right) \quad \text{----- (10)}$$

The calculated yield strength is equal to 193.55 MPa for LPPS single crystal. The hardness parameters are listed in Table 4.

Table 4 Hardness data of LPPS crystal

Crystal	n	k_1 (kg/mm ²)	k_2 (kg/mm ²)	x (μ m)	σ_v (MPa)
LPPS	2.85	621.55	77.01	10.7	193.55

The elastic stiffness constant (C_{11}) for different loads are calculated using Wooster’s empirical formula $C_{11} = H_v^{7/4}$ and is shown in Table 5. The stiffness constant gives an idea about the tightness of bonding with the neighboring atoms. In the case of LPPS crystal, the stiffness constant is found to increase with the applied load.

Table 5 Elastic stiffness constant for different loads

Load (g)	C_{11} (10 ¹⁴ Pa)
25	1257.87
50	2187.00
100	5470.85

Conclusion

Optical quality single crystals of LPPS were grown using solution growth technique. Compound confirmation was done by energy-dispersive spectrometry. The unit-cell parameters of LPPS were determined by single crystal X-ray diffraction analysis. The thermal behavior of the grown crystals was studied by using Thermo Gravimetric analysis. The functional groups present in the sample were confirmed by FTIR. In the transmittance spectra, it is evident that the LPPS crystal has a wide transparency range in the entire visible range. The SHG relative efficiency of LPPS is 0.67 times that of KDP. Thus, LPPS seems to be a promising material for NLO application. From the mechanical measurements, it is observed that the hardness increases with increase of load. The elastic stiffness constant for LPPS has been reported. The optical band gap (E_g), absorption coefficient (α), and extinction coefficient (K) were also calculated as a function of wavelength.

Acknowledgment

The authors would like to thank the staff members of RRL (Trivandrum), Crescent Engineering College (Chennai), STIC (Cochin) and M.K. University (Madurai) for having helped us to carry out the research work. Also we thank authorities of Management of Aditanar College of Arts and Science, Tiruchendur, Govindammal Aditanar College for Women, Tiruchendur and S.T. Hindu College, Nagercoil for the encouragement given to us to carry out the research work.

References

1. Chemla J.D and Zyss (Eds.) S., Nonlinear Optical Properties of Organic Molecules and Crystals, 1, (London: Academic Press), 1987.
2. Prasad P. N. and Williams D.J., Introduction to Nonlinear Optical Effects in Molecules and Polymers, (New York : Wiley-Interscience), 1991.
3. Xu. D. and Xue D., Chemical bond simulation of KADP single crystal growth. J. Crystal Growth, 2008, 310, 1385-1390.
4. Yu D., Xue D. and Ratajczak H., Bond-valence parameters for characterizing O–H–O hydrogen bonds in hydrated borates, 2006, J. Mol. Struc. 792–793, 280–285.
5. Xu D. and Xue D., Chemical bond analysis of the crystal growth of KDP and ADP, J. Cryst. Growth, 2006, 286, 108-113.
6. Narayan Bhat M. and Dharmaprakash S.M., New nonlinear optical material: glycine sodium nitrate, J. Cryst. Growth, 2002, 235, 511-516.
7. Deepthy A. and Bhat H.L., Growth and characterization of ferroelectric glycine phosphite single crystals, 2001 J. Cryst. Growth 226, 287-293.
8. Rajasekaran R., Ushashree P.M., Jayavel R. and Ramasamy P., Growth and characterization of zinc thiourea chloride(ZTC) –a semiorganic nonlinear optical crystal, J. Cryst. Growth, 2001, 229, 563-567.
9. Lydia Caroline M. and Vasudevan S., Growth and characterization of an organic nonlinear optical material:L-alanine alaninium nitrate, Mater. Lett., 2008, 62, 2245-2248.
10. Frankenbach G.M. and Etter M.C., Relationship between symmetry in hydrogen-bonded benzoic acids and the formation of acentric crystal structures,Chem. Mater., 1992, 4, 272-278.
11. Etter M.C. and Huang K.S., Induction of noncentrosymmetry by polar hydrogen-bonded chains in nitroaniline crystals, Chem. Mater 4, 1992, 824-827.
12. Sarma J.A.N.R.P., Dhurjati M.S.K., Ravikumar I.C. and Bhanuprakash K., Molecular and Crystal Engineering Studies of Two 2, 4-Dinitroalkoxystilbenes: An Endeavor To Generate Efficient SHG Crystal, Chem. Mater., 1994, 6, 1369-1377.
13. Myung S., Pink M., Baik M.H. and David Clemmer E., DL-Proline. Acta Crystallography C, 2005, 61, 506-508.
14. Boomadevi S. and Dhanasekaran R., Synthesis, crystal growth and characterization of L-pyrrolidone -2 -carboxylic acid (L-PCA) crystal, J. Crystal Growth, 2004, 261, 70-76.
15. Uma Devi T., Lawrence N., Ramesh Babu R. and Ramamurthi K., Growth and Characterization of L-prolinium picrate single crystal: A promising NLO crystal, J. Crystal Growth, 2008 310, 116-123.
16. Thomas Joseph Prakash J. and Kumararaman S., Growth and characterization of L-proline cadmium chloridemonohydrate single crystals, Materials Letters, 2008 62, 4097-4099.
17. Suresh S., Ramanand A., Jayaraman D. and Mani P., Dielectric studies of L-Prolinium Tartrate (LPT) NLO Single crystals, Journal of optoelectronics and Advanced materials, 2010, 4, 1743-1746.
18. Anandha Babu G. and Ramasamy P., Synthesis, crystal growth and characterization of novel semiorganic nonlinear optical crystal: Dichlorobis (l-proline) zinc (II), Materials Chemistry and Physics, 2009, 113, 727-733.
19. UmaDevi T., Lawrence N., Ramesh Babu R., Selvanayagam S, Helen Stoeckli- Evans and Ramamurthi K., Synthesis, Crystal Growth and Characterization of L-Proline Lithium Chloride Monohydrate: A New Semiorganic Nonlinear Optical Material, Cryst. Growth Des., 2009, 9(3), 1370-1374.
20. Selvarajan P., Sivadhas A., Freeda T. H. and Mahadevan C. K., Growth, XRD and Dielectric studies of Triglycine sulpho-phosphate (TGSP) crystals added with magnesium sulphate, Phys.B, 2008, 403, 4205.

21. Theresita Shanthi N., Selvarajan P. and Mahadevan C. K., Growth, Structural, mechanical, spectral and dielectric characterization of NaCl-added Triglycine sulphate single crystals, *Curr. Appl. Phys.*, 2009, 9, 1155-1159.
22. Lipson H. and Steeple M., *Interpretation of X-ray Powder Diffraction Patterns*, (Newyork: McMillan) 1970.
23. Lydia Caroline M., Kandasamy A., Mohan R. and Vasudevan S., Growth and Characterization of dichlorobis L-proline Zn (II): A semiorganic nonlinear optical single Crystal, *J. Cryst. Growth*, 2009, 311, 1161-1165.
24. Balakrishnan T. and Ramamurthi K., Growth, structural, optical, thermal and mechanical properties of glycine zinc chloride single crystal, *Material Letters*, 2008, 62, 65-68.
25. Lucia Rose A. S. J., Selvarajan P. and Perumal S., Growth, structural, spectral, mechanical, thermal and dielectric characterization of phosphoric acid admixed L-alanine (PLA) single crystals, *Spectrochimica Acta Part A: Molecular and Biomolecular Spectroscopy*, **2011**, 81, 270-275.
26. Azha. Periasamy, Muruganand S. and Palaniswamy M., Vibrational studies of Na₂SO₄,K₂SO₄, NaHSO₄ and KHSO₄ crystals, *RASAYAN J. Chem*, 2009, 2(4), 981-989.
27. Krishnan S., Justin Raj C., Navis Priya S.M., Robert R., Dinakaran S. and Jerome Das S., Optical and dielectric studies on succinic acid single crystals. *Cryst. Res. Technol*, 2009 43, 845-850.
28. Onitsch E.M., *Mikroskopie*, 1947, 2, 131-151.
29. Hanneman M., *Metall, Manch*, 1941, 23, 135-139.
30. Vela T., Selvarajan P., Freeda T.H. and Balasubramanian K., Growth and characterization of pure and semiorganic nonlinear optical Lithium Sulphate admixed L-alanine crystal. *Physica Scripta*, 2013, 87, 045801.
31. Vesta C., Uthrakumar R., Justin Raj C., Jonie Varjula A., Mary Linet J. and Jerome Das S., Growth, Structural and Microhardness Studies on New Semiorganic Single Crystals of Calcium Para Nitrophenolate Dihydrate, *Journal of Material and Scientific Technologies*, 2007, 23, 855-859.
32. Chako E., Mary Linet J., Navis Priya S.M., Vesta C. , Milton Boaz B. and Jerome Das S., Growth, Structural, Optical, Mechanical and Dielectric Characterization of Diammonium Hydrogen Phosphate (DAHP) Single Crystals, *Indian Journal of Pure and Applied Physics*, 2004, 44, 260-263.
